Light Emission from the Slow Mode of Tunnel Junctions on Short Period Diffraction Gratings

P. D. Sparks, T. Sjodin, B. W. Reed, and J. Stege
Department of Physics, Harvey Mudd College, Claremont, California 91711
(Received 4 February 1992)

The emission of light from metal-oxide-metal tunnel junctions has been studied as a probe of the interaction of the tunneling current with the surface plasmon polaritons of the tunnel junction structure. The slow mode, with large fields in the oxide layer, is most directly coupled to the tunneling current. In this experiment, diffraction gratings with periods between 70 and 100 nm provide the momentum for the slow mode to radiate. We report the unambiguous measurement of the direct emission from the slow mode showing that it does contribute to the light emission.

PACS numbers: 73.40.Rw, 73.40.Gk

The emission of light from metal-oxide-metal tunnel junctions was first reported by Lambe and McCarthy [1] in 1976. They identified a particular surface plasmon polariton (SPP) as the source of the light and argued that the mode was driven by inelastic tunneling current fluctuations. Many experiments have been done on these structures, and quantitative theories have been developed to explain the results [2–5]. The discussion centers on two questions: the identification of the SPP mode which dominates the intermediate step in the light emission, and the driving mechanism for that mode.

There are three SPP modes in the visible supported by a typical Al-oxide-Au tunnel junction [6]. The Au fast mode has its largest field amplitudes on the Au-air interface. For this mode, at any energy in the visible, the component of the wave vector of the SPP in the plane of the junction, $k_{\parallel}$, is about twice the free-space wave vector of the emitted light. The radiation associated with the fast mode has been observed from junctions grown on gratings [7–9] and junctions formed on prisms [3,6,10]. The required period of the grating is set by the mismatch between $k_{\parallel}$ of the SPP and the k for the emitted light. For the fast mode, the gratings had periods of approximately 800 nm. There is also an Al-substrate fast mode, which is not important in the discussion of the light emission [11].

The third SPP mode is the slow mode. It has its largest field amplitudes in the oxide layer. For energies in the visible, $k_{\parallel}$ for the slow mode is roughly an order of magnitude larger than that for the fast mode. There is evidence for light emission from randomly rough junctions through the decay of the slow mode [11–13]. To observe the radiation from the slow mode directly, it is necessary to couple to the SPP via a diffraction grating with a very short period: approximately 80 nm. The direct measurements of the slow mode are reported in this paper.

Sample fabrication.—The samples were formed at the National Nanofabrication Facility (NNF) at Cornell University. The substrates were silicon wafers with a thermally grown 100-nm oxide. Grating patterns with periods of 70, 85, and 100 nm were exposed by electron beam nanolithography using a JEOL JBX 5DIIU system. An area of 200 μm×200 μm was exposed in sixteen sections. For the purposes of this experiment, the registry between adjacent sections is unimportant because the coherence length of the slow mode is less than these lateral dimensions. The image was transferred to the underlying SiO_2 by reactive ion etching using SF_6 and CHF_3 gases. The etch depth was measured to be 27 ± 3 nm. A scanning electron microscope image of a coprocessed grating with a period d of 70 nm is shown in Fig. 1.

After the gratings were fabricated, the tunnel junctions were formed using thermal evaporations and contact photolithography. The Al film thickness was 60 nm for the junction shown on a 70-nm-period grating and 55 nm for the junctions on the 85- and 100-nm-period gratings.

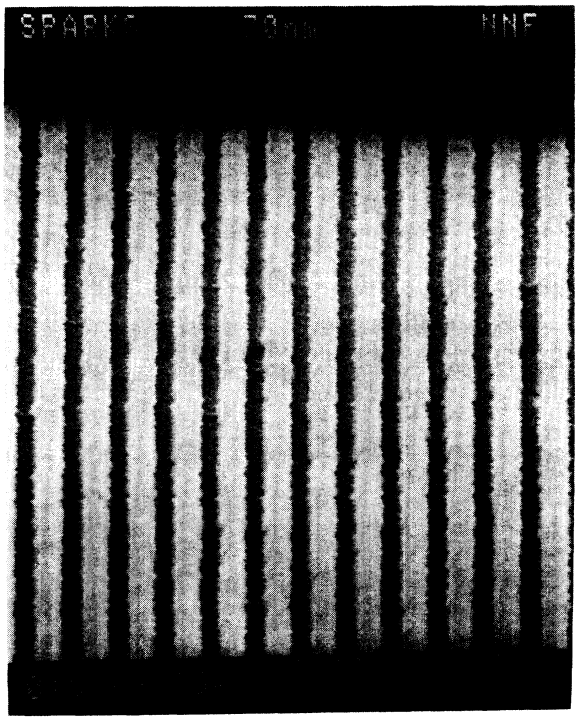

FIG. 1. Scanning electron microscope image of a 70-nm-period grating in SiO_2. The profile is of approximately 10 nm of resist and 30 nm etched into the SiO_2.

The Al films were oxidized in air at 200°C for 30 min. In removing the photoresist from the Al, the Al was exposed to an oxygen plasma. This step may have produced a thicker oxide than the thermal growth step did. The Au film thickness was 30 nm.

The tunnel junctions were examined with an optical microscopic after fabrication. It was clear that they were aligned with the underlying grating to within approximately 2 μm out of the 200-μm extension. The fact that the damage on the SiO_2 due to the e-beam lithography was visible through the Au film indicates that the grating structure penetrated through the junction. Tunnel junctions on identical substrates but without gratings were made at the same time.

Optical measurements.—Light emission is measured using a SPEX 500M grating spectrometer, a Hamamatsu R943-02 photomultiplier, and photon-counting electronics with a resolution in wavelength of 4.8 nm. The collection optics consist of achromatic lenses and a Glan-Thompson polarizer. All the light in a cone of half-angle 18° (0.32 sr) about the direction normal to the plane of the junctions is accepted. The observed spectral distribution does not change when the acceptance angle is decreased to 9°. The optical system is calibrated with an Optronics Model 300 low-light-level calibration source by passing the known light output through the collection optics.

Because the light from the tunnel junctions is a mixture of linear polarizations, the calibrations and data acquisition are done separately for two orthogonal polarizations. To define the geometry, suppose the optical axis is along **x** and the junction is in the y-z plane with the lines of the grating parallel to the **z** axis. The SPPs traveling perpendicular to the grating will have fields with $\mathbf{E} = E_y\mathbf{y} + E_x\mathbf{x}$ and $E_z = 0$. We will refer to the two polarization components as **Y**, for light with $E_z = 0$, and **Z**, for light with $E_y = 0$. The light emitted by the decay of the SPPs mediated by the grating will have the **Y** polarization.

The raw data for count rate per unit wavelength versus wavelength are corrected for the detection efficiency. The data are then normalized by the current and the solid angle. The units are thus photons per electron per unit photon energy per steradian. Any two of the measured spectra can be directly compared to establish their relative efficiency.

The tunnel junctions are voltage biased by an active circuit. The measurements are made with the junctions in air at room temperature. The bias current, used to normalize the spectra, was stable during the data acquisition. Typical currents were 75 μA at 3.0-V bias for a current density of 0.19 A/cm^2. The peak count rate averaged 40 (counts/s) μA. The junctions were biased at 3.0 V for all the spectra shown.

Results.—The spectra for the two polarizations of light from a tunnel junction on a diffraction grating with a period of 85 nm is shown in Fig. 2. The two spectra are markedly different, with features shared by the spectra from all the junctions. The **Z** polarization for all junctions consists of a broad background with a peak near 2.0 eV and a full width at half maximum (FWHM) of about 1 eV. The shapes are identical and the magnitudes vary by a factor of 2, which is within typical sample-to-sample variations for light-emitting tunnel junctions. Furthermore, the spectral distribution for this component is the same as that for light from the junctions with no underlying gratings. We conclude that the Z component arises from the unpolarized light emitted when SPPs scatter off the residual roughness.

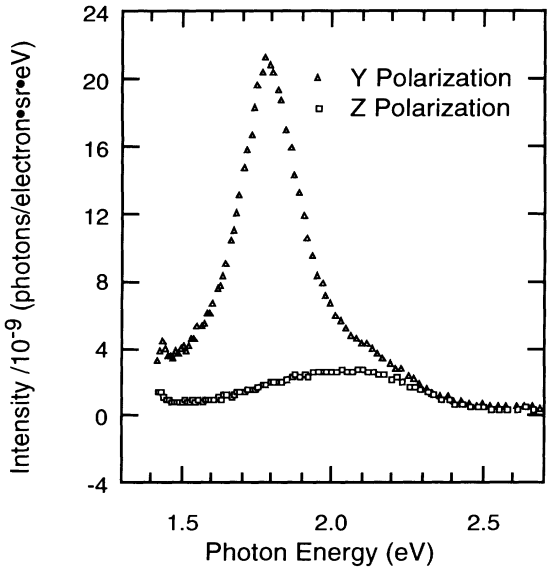

FIG. 2. Spectrum of light taken off the Au side of a junction grown on an 85-nm-period grating. The current was 66 μA. The **Y** polarization has its electric field perpendicular to the lines of the grating. The **Z** polarization has its electric field parallel to the lines of the grating. For all the spectra, the error bars are comparable to the scatter in the points or the symbol size.

The **Y** polarization in Fig. 2 shows a sharp peak with a FWHM ≈ 0.25 eV superposed on the broadband emission. The polarization of the sharp peaks is consistent with the scattering of SPPs off the gratings. The peak position varies with the periodicity of the grating: As the period d decreases, the momentum transfer in scattering, $2\pi/d$, increases, and SPPs with larger values of $k_\parallel$ can scatter into the normal direction. Since larger $k_\parallel$ corresponds to higher energy, the peak energy increases for decreasing period.

We have assumed that the **Y** polarization includes a contribution from the scattering off the random roughness that is equal in magnitude to the measured **Z** component. Subtracting the **Z** component from the **Y** component yields a signal due only to the scattering off the diffraction grating. This difference signal is plotted in Figs. 3–5 for gratings with periods of 70, 85, and 100 nm, respectively. Each spectrum contains a sharp peak. We

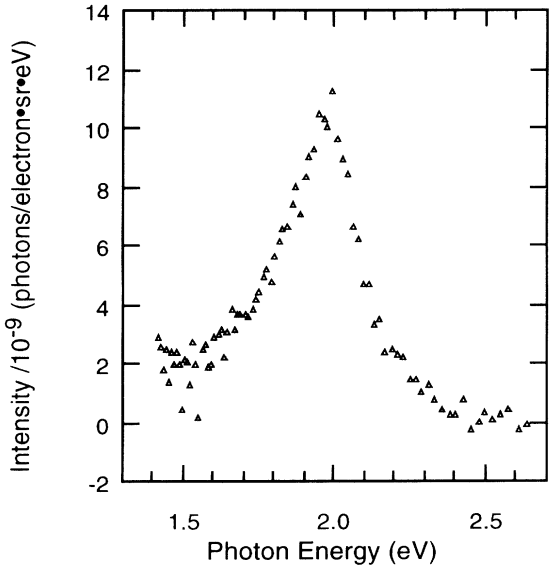

FIG. 3. Spectrum for the difference in the Y and Z polarizations to isolate the scattering off the grating for a junction on a 70-nm-period grating. The current was 15 μA.

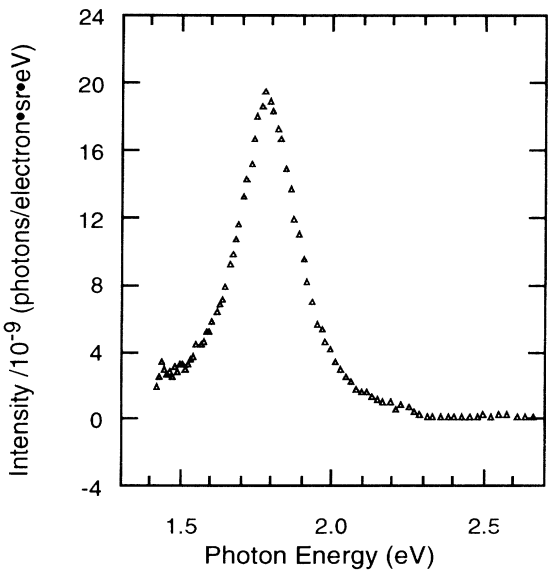

FIG. 4. Spectrum for the difference in the Y and Z polarizations to isolate the scattering off the grating for a junction on an 85-nm-period grating. The current was 66 μA.

identify these peaks as evidence for the radiative decay of the slow mode.

The calculations by Sparks and Rutledge [11] show the response of the slow mode to the driving current. For any $k_{\parallel}$, the energy at which the value of $|E_y|^2$ is a maximum determines the energy at which the emission from the slow mode would peak for scattering normal to the junction. In Table I the measured energies of the sharp peaks are compared with the calculated maxima. There is a remarkable agreement for the junctions reported here. It is known [14] that the dispersion relation for the slow mode depends on the oxide thickness. For thicker oxides, the dispersion relation shifts to lower values of $k_{\parallel}$. In this experiment, that would correspond to higher peak energies for any particular grating. The data are consistent with the oxide thickness for our samples being thicker than the 3 nm used in the calculations.

The broad background subtracts cleanly from the spectra in Figs. 3 and 4 for the 70- and 85-nm-period gratings. The junctions on the 100-nm-period gratings, however, showed a peak near 2.0 eV that cannot be attributed to unpolarized light from the residual roughness. The energy for this peak is consistent with the energy for second-order scattering off the grating. It is possible that the grating profiles for the 100-nm-period grating are sufficiently different from those for the shorter period gratings to change the relative importance of the second-order scattering. This excess polarized light will be further investigated.

The absolute quantum efficiencies shown in Table I were found by integrating the spectrum over all energies. These numbers are for radiation normal to the gratings at room temperature only. For a related system, Kirtley *et al.* found typical efficiencies for the decay of the fast mode on cold Al-oxide-Ag tunnel junctions on gratings to be in the range of 2×10^{-9} to 3×10^{-7} photons/electron sr [8]. Their efficiencies were 50% lower at room temperature [7]. For a direct comparison to the results of Kirtley *et al.*, it is necessary to divide our data by a factor of order $(1-\hbar\omega/eV_0)/2\pi$ to account for the relative amplitude of the inelastic scattering components driving the

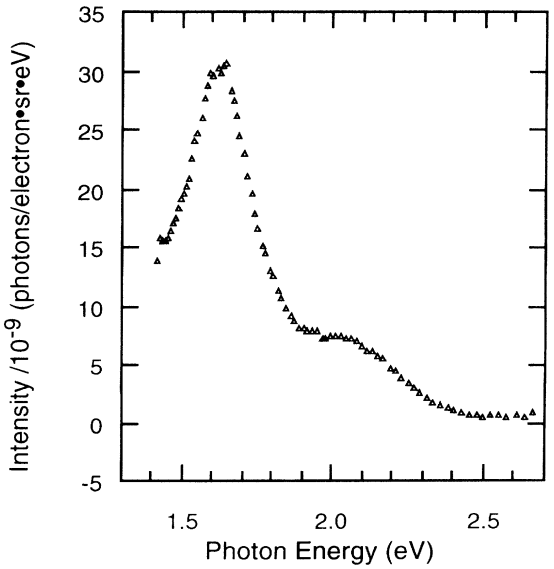

FIG. 5. Spectrum for the difference in the Y and Z polarizations to isolate the scattering off the grating for a junction on a 100-nm-period grating. The current was 85 μA.

TABLE I. Measurements on the peaks from the slow mode on three diffraction grating periods.

Period (nm)	E_{max} (measured) (eV)	E_{max} (estimated) [a] (eV)	Quantum efficiency (photons/electron sr)
70	1.97	1.86	4.2×10^{-9}
85	1.79	1.72	5.7×10^{-9}
100	1.62	1.57	1.2×10^{-8}

[a]Reference [10].

SPPs. The effect of that correction is to multiply our efficiencies by approximately 15. In addition, the slow mode radiation is into a large solid angle, whereas the emission from the fast mode is into a narrow angular range. Thus in terms of total light output, the slow mode is brighter.

This paper does not address directly the origin of the unpolarized broadband radiation. However, the evidence that the slow mode can decay optically provides further support for the conclusion that the slow mode dominates the light emission from residually rough junctions.

We report the unambiguous observation of light emission from the slow mode in Al-oxide-Au tunnel junctions. The ability to use short period gratings to analyze the direct contribution of the slow mode to the light emission provides an exciting method of making stringent tests on the inelastic tunneling models for the excitation of this mode. These experiments probe the optical properties of structures on a length scale between that for a conventional grating and that for a scanning tunneling microscope tip. Further experiments will define the dispersion relation for the slow mode and examine the effects on the quantum efficiency of the grating height.

This work was performed at Harvey Mudd College and the National Nanofabrication Facility, Cornell University. It was supported, in part, by the Research Corporation under Grant No. C-2950, the National Science Foundation (NSF) Research in Undergraduate Institutions Program under Grant No. DMR-9002023, the NSF Improvements in Laboratory Instrumentation Program under Grant No. USE-9152537, and the Harvey Mudd Research Committee. The National Nanofabrication Facility is supported by the NSF under Grant No. ECS 8619049. We thank the staff at the NNF, in particular, Richard Tiberio. We also thank past students M. Albee, S. Applebaum, J. Guild, D. Richards, C. Sackett, and P. Varekamp for helping assemble the equipment at HMC and thank J. E. Rutledge for useful conversations. This experiment could not have been performed without the advice and the equipment of J. Eckert and W. Sandmann.

[1] J. Lambe and S. L. McCarthy, Phys. Rev. Lett. **37**, 923 (1976).

[2] A useful set of references for work done before 1984 appears in P. Dawson, D. G. Walmsley, H. A. Quinn, and A. J. L. Ferguson, Phys. Rev. B **30**, 3164 (1984).

[3] More recent developments are referenced in K. Suzuki, J. Watanabe, A. Takeuchi, Y. Uehara, and S. Ushioda, Solid State Commun. **69**, 35 (1989).

[4] For light emission from the STM geometry, J. K. Gimzewski, B. Reihl, J. H. Coombs, and R. R. Schlittler, Z. Phys. **72**, 497 (1988), and references therein.

[5] B. Laks and D. L. Mills, Phys. Rev. B **20**, 4962 (1979); **21**, 5175 (1980); **22**, 5723 (1980).

[6] S. Ushioda, J. E. Rutledge, and R. M. Pierce, Phys. Rev. B **34**, 6804 (1986).

[7] John Kirtley, T. N Theis, and J. C. Tsang, Phys. Rev. B **24**, 5650 (1981).

[8] J. R. Kirtley, T. N Theis, J. C. Tsang, and D. J. Di Maria, Phys. Rev. B **27**, 4601 (1983).

[9] N. Kroó, Zs. Szentirmay, and J. Félszerfalvi, Phys. Lett. **88A**, 90 (1982).

[10] J. Watanabe, A. Takeuchi, Y. Uehara, and S. Ushioda, Phys. Rev. B **38**, 12959 (1988).

[11] P. D. Sparks and J. E. Rutledge, Phys. Rev. B **40**, 7574 (1989).

[12] S. Ushioda, J. Lumin. **47**, 131 (1991).

[13] The paper by H. P. Hagan, A. J. L. Ferguson, R. J. Turner, K. W. Smith, P. Dawson, and D. G. Walmsley [J. Vac. Sci. Technol. B **9**, 879 (1991)] contradicts the conclusion of the importance of the slow mode. We believe their measurements of surface annealing are not relevant, because the length scale is an order of magnitude too small, and the roughness at the *oxide metal* interface determines the slow mode scattering.

[14] J. B. D. Soole and C. D. Ager, J. Appl. Phys. **65**, 1133 (1989).

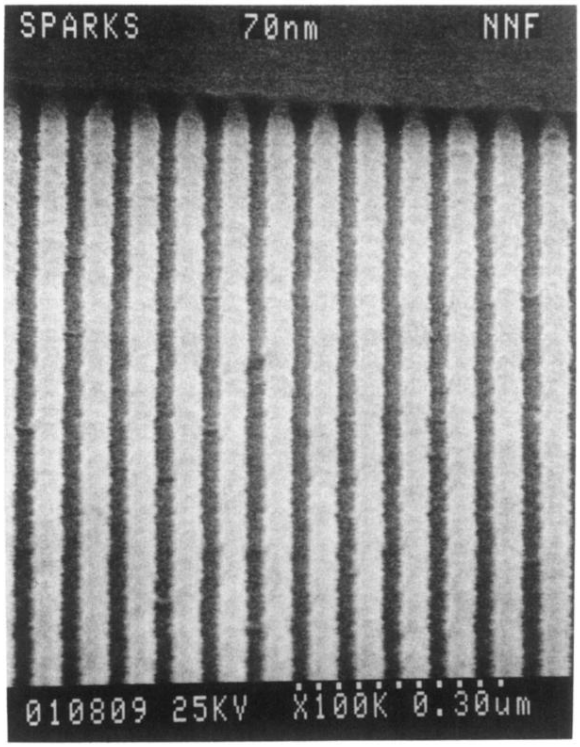

FIG. 1. Scanning electron microscope image of a 70-nm-period grating in SiO_2. The profile is of approximately 10 nm of resist and 30 nm etched into the SiO_2.